Intracellular and Extracellular Concentrations of Na^+ Modulate Mg^{2+} Transport in Rat Ventricular Myocytes

Michiko Tashiro, Pulat Tursun, and Masato Konishi
Department of Physiology, Tokyo Medical University, Tokyo 160-8402, Japan

ABSTRACT Apparent free cytoplasmic concentrations of Mg^{2+} ($[Mg^{2+}]_i$) and Na^+ ($[Na^+]_i$) were estimated in rat ventricular myocytes using fluorescent indicators, furaptra (mag-fura-2) for Mg^{2+} and sodium-binding benzofuran isophthalate for Na^+, at 25°C in Ca^{2+}-free conditions. Analysis included corrections for the influence of Na^+ on furaptra fluorescence found in vitro and in vivo. The myocytes were loaded with Mg^{2+} in a solution containing 24 mM Mg^{2+} either in the presence of 106 mM Na^+ plus 1 mM ouabain (Na^+ loading) or in the presence of only 1.6 mM Na^+ to deplete the cells of Na^+ (Na^+ depletion). The initial rate of decrease in $[Mg^{2+}]_i$ from the Mg^{2+}-loaded cells was estimated in the presence of 140 mM Na^+ and 1 mM Mg^{2+} as an index of the rate of extracellular Na^+-dependent Mg^{2+} efflux. Average $[Na^+]_i$, when estimated from sodium-binding benzofuran isophthalate fluorescence in separate experiments, increased from 12 to 31 mM and 47 mM after Na^+ loading for 1 and 3 h, respectively, and decreased to ~0 mM after 3 h of Na^+ depletion. The intracellular Na^+ loading significantly reduced the initial rate of decrease in $[Mg^{2+}]_i$, on average, by 40% at 1 h and by 64% at 3 h, suggesting that the Mg^{2+} efflux was inhibited by intracellular Na^+ with 50% inhibition at ~40 mM. A reduction of the rate of Mg^{2+} efflux was also observed when Na^+ was introduced into the cells through the amphotericin B-perforated cell membrane (perforated patch-clamp technique) via a patch pipette that contained 130 mM Na^+. When the cells were heavily loaded with Na^+ with ouabain in combination with intracellular perfusion from the patch pipette containing 130 mM Na^+, removal of extracellular Na^+ caused an increase in $[Mg^{2+}]_i$, albeit at a very limited rate, which could be interpreted as reversal of the Mg^{2+} transport, i.e., Mg^{2+} influx driven by reversed Na^+ gradient. Extracellular Na^+ dependence of the rate of Mg^{2+} efflux revealed that the Mg^{2+} efflux was activated by extracellular Na^+ with half-maximal activation at 55 mM. These results contribute to a quantitative characterization of the Na^+-Mg^{2+} exchange in cardiac myocytes.

INTRODUCTION

Cytoplasmic free $[Mg^{2+}]$ ($[Mg^{2+}]_c$) significantly influences numerous functions in muscle cells including enzymatic activities (e.g., ATPases), K^+ and Ca^{2+} channels (1,2), excitation-contraction coupling (3), Ca^{2+} sensitivity of myofilaments (4), and Ca^{2+} binding to intracellular sites (5,6). In cardiac myocytes, $[Mg^{2+}]_c$ is maintained within the 0.8–1.0-mM range (7,8). $[Mg^{2+}]_c$ is thought to be regulated by the balance between passive influx driven by the electrochemical gradient and active extrusion. Because a major part of the active Mg^{2+} extrusion appears to require extracellular Na^+ in cardiac myocytes (9–11), as well as in other cells, Na^+-Mg^{2+} exchange (i.e., Mg^{2+} efflux coupled with Na^+ influx) has been postulated as the major Mg^{2+} extrusion pathway (12–14). However, the properties of the transport have not been completely characterized.

We have previously described modulation of Na^+-dependent Mg^{2+} efflux in rat ventricular myocytes by cytoplasmic and extracellular Mg^{2+} concentration ($[Mg^{2+}]_c$ and $[Mg^{2+}]_o$, respectively). The efflux is activated by a slight elevation of $[Mg^{2+}]_c$ above the basal level (~0.9 mM) with half-maximal activation at 1.9 mM $[Mg^{2+}]_c$, whereas it is inhibited by high $[Mg^{2+}]_o$ with 50% inhibition at ~10 mM (8). This study focuses on the modulation of Mg^{2+} efflux by cytoplasmic and extracellular concentrations of Na^+ ($[Na^+]_c$ and $[Na^+]_o$, respectively). The technique relies on fluorescent indicators for Mg^{2+} (furaptra) and Na^+ (sodium-binding benzofuran isophthalate (SBFI)). The Mg^{2+} efflux rate was estimated in cells depleted of intracellular Na^+ by extracellular perfusion with an essentially Na^+-free solution, and in cells that had been loaded with Na^+ by application of ouabain. In some experiments, $[Na^+]_c$ was directly manipulated by intracellular perfusion from a patch pipette through amphotericin B-perforated cell membrane (perforated patch-clamp technique). We also explored the possibility that a reversed Na^+ gradient could drive Mg^{2+} influx.

Some of the results have appeared in abstract form (15).

METHODS

General

The experimental techniques used in this study, as well as the setup have been described previously (8,16). Briefly, single ventricular myocytes enzymatically isolated from male rat hearts (Wistar, 9–12 weeks) were placed in a superfusion bath on the stage of an inverted microscope (TE300; Nikon, Tokyo, Japan) and superfused with normal Tyrode's solution composed of (in millimolar): 135 NaCl, 5.4 KCl, 1.0 $CaCl_2$, 1.0 $MgCl_2$, 0.33 NaH_2PO_4, 5.0 glucose, and 10 HEPES (pH 7.40 at 25°C by NaOH). After the background fluorescence (cell autofluorescence plus instrumental stray fluorescence) was measured, the cells were incubated at room temperature

Submitted June 16, 2005, and accepted for publication July 18, 2005.

Address reprint requests to Dr. Masato Konishi, Dept. of Physiology, Tokyo Medical University, 6-1-1 Shinjuku, Shinjuku-ku Tokyo 160-8402, Japan. Tel.: 81-3-3351-6141; Fax: 81-3-5379-0658; E-mail: mkonishi@tokyo-med.ac.jp.

0006-3495/05/11/3235/13 $2.00

doi: 10.1529/biophysj.105.068890

with either 5 μM furaptra AM for 13–15 min or 20 μM SBFI AM plus 0.02% pluronic for 2 h. The AM ester of the indicator was then washed out with Ca-free Tyrode's solution (which contained 0.1 mM K_2EGTA in place of the 1.0 mM $CaCl_2$ of normal Tyrode's solution; Table 1), and subsequent measurements of the indicator fluorescence were carried out at 25°C in Ca^{2+}-free conditions. Use of Ca^{2+}-free solutions should help minimize any potential interference in furaptra's fluorescence signal by changes in cytoplasmic $[Ca^{2+}]$ ($[Ca^{2+}]_c$). Fluorescence intensity at 500 nm was measured from single cells with illumination wavelengths of 350 and 382 nm for furaptra, and 340 and 382 nm for SBFI. At each illumination wavelength, the background fluorescence was subtracted from the total fluorescence measured after the indicator loading to give indicator fluorescence intensity at each wavelength, and thereby the ratio of the indicator fluorescence intensities (R). For the perforated patch-clamp experiments with furaptra (see below), in which the background fluorescence was not measured from the same cells, intensities of the background fluorescence were measured without indicator loading from 3 to 5 myocytes with a size (length × width) similar to that used for the experiments, and the average value at each excitation wavelength was subtracted from the total fluorescence to give indicator fluorescence intensity (8). Note that small cell-to-cell variation of the autofluorescence should have little influence on the estimated $[Mg^{2+}]_i$, because cell autofluorescence typically represents only a few percent of furaptra fluorescence.

Calibration of furaptra signals

The ratio of furaptra fluorescence intensities excited at 382 nm (a Mg^{2+}-sensitive wavelength) and 350 nm (an isosbestic wavelength) was used as a Mg^{2+}-related signal [furaptra $R = F(382)/F(350)$]. With identical optical conditions, a slow rise of furaptra R was observed during the course of this study, which was conducted over a 20-month period. This was likely due to aging of the lamp and other optical components. To correct for the slow drift, we occasionally (typically once a week) measured R under standard conditions. For this standard, we used 50 μM furaptra in a Ca^{2+}-Mg^{2+}-free buffer solution (140 mM KCl, 10 mM NaCl, 1 mM EDTA, 1 mM EGTA, 10 mM PIPES, pH 7.1); thin-wall quartz capillaries (internal diameter ~50 μm) that contained the indicator solution were placed in the superfusion bath and R was measured. All R values measured from cells were normalized to the standard R, and the normalized R was converted to $[Mg^{2+}]_i$ according to the equation:

$$[Mg^{2+}]_i = K_D \frac{R - R_{min}}{R_{max} - R}, \quad (1)$$

where R_{min} and R_{max} are the normalized R values at zero $[Mg^{2+}]_i$ and saturating $[Mg^{2+}]_i$, respectively, and K_D is the dissociation constant. We used the parameter values previously estimated in rat ventricular myocytes at 25°C: $R_{min} = 0.969$, $R_{max} = 0.223$, and $K_D = 5.30$ mM (17). The method depends on construction of a calibration curve in the cells treated with ionophores (ionomycin, monensin, nigericin, and valinomycin), in which Mg^{2+} is thought to be distributed uniformly throughout the cytoplasm and intracellular organelles. In intact myocytes, on the other hand, ~22% of furaptra molecules in the myocytes are localized in intracellular organelles (primarily mitochondria) after AM loading, and the apparent $[Mg^{2+}]$ in the organelles appears to be maintained within the 0.6–0.7 mM range irrespective of $[Mg^{2+}]_c$ between 0.8 and 4.0 mM (8). Thus, $[Mg^{2+}]_i$ (i.e., apparent cytoplasmic $[Mg^{2+}]$) estimated as the spatially averaged Mg^{2+} concentration from the entire cell volume may not reflect $[Mg^{2+}]_c$ only. Possible errors associated with compartmentation of furaptra are considered below.

Calibration of SBFI signals

The ratio of SBFI fluorescence intensities excited at 382 nm [$F(382)$] and 340 nm [SBFI $R = F(382)/(340)$] was corrected for the slow instrumental drift by normalization to a standard R, as described above for furaptra. As the standard for SBFI R, we used quartz capillaries (see above) containing 50 μM fura-2 dissolved in the Ca^{2+}-Mg^{2+}-free buffer solution. All measured values of R from the cells were normalized to the standard R, which was then converted to $[Na^+]_i$ with an equation analogous to Eq. 1, as described in the next paragraph.

Fig. 1 illustrates intracellular calibration of SBFI fluorescence in terms of $[Na^+]_i$ in solutions with a composition similar to that described by Harrison et al. (1992): 0–130 mM NaCl plus 130–0 mM KCl (Na^+ and K^+ were varied reciprocally), 10 mM K_2EGTA, 5 mM glucose, 1 mM ouabain, 1 mg/l gramicidin D, and 5 mM HEPES (pH 7.1 by KOH). Gramicidin D was included to permeabilize the cell membrane to small cations (18). When $[Na^+]_o$ was reduced from 140 mM (Ca^{2+}-free Tyrode's solution) to 0 mM and then increased stepwise to 100 mM (Fig. 1 *A*), $F(382)$ of SBFI increased and then decreased stepwise, respectively, as expected for corresponding increases then decreases in $[Na^+]_i$. On the other hand, $F(340)$ stayed relatively constant (Fig. 1 *A*) irrespective of $[Na^+]_o$ between 0 and 140 mM. This observation is in agreement with the finding by Donoso et al. (19), and suggests that 340 nm is very close to an isosbestic wavelength of intracellular SBFI for Na^+. The nearly constant $F(340)$ at different $[Na^+]_i$ justified the use of a simple equation of the same form as Eq. 1 for calibration of the SBFI R signal. The relation between $[Na^+]_i$ and SBFI R was obtained under the assumption that, in the presence of gramicidin D in the divalent cation-free solutions, $[Na^+]_i$ reached the same level as $[Na^+]_o$ (Fig. 1 *B*). These data were least-squares fitted using a theoretical 1:1 binding curve with the same form as Eq. 1. The calibration curve and parameter values thus obtained are shown in Fig. 1 *B*.

Although a significant fraction of SBFI molecules (e.g., ~50% (19)) loaded into cardiac myocytes is likely localized inside intracellular organelles, the intracellular calibration curve should still be valid for estimation of $[Na^+]_c$, unless distribution of SBFI and Na^+ was affected by gramicidin D.

TABLE 1 Pipette and extracellular solutions

Pipette solutions (mM)	KMs	NaMs	KCl	NaCl	$CaMs_2$	$MgMs_2$	MOPS		$[Na^+]$	$[K^+]$
145 K/0 Na	130	0	10	0	1.0	1.0	10		0	145
130 Na/15 K	13	117	1	9	1.0	1.0	10		130	15
Extracellular solutions (mM)	**NaCl**	**KCl**	**NMDG**	**$MgCl_2$**	**$MgMs_2$**	**K_2EGTA**	**NaH_2PO_4**	**HEPES**	**Glucose**	**Ouabain**
Ca-free Tyrode's	135	5.4	0	1.0	0	0.1	0.33	10	5	0
NMDG Tyrode's	0	5.4	135	1.0	0	0.1	0.33	10	5	0
Na-loading	101	5.4	0	17.9	6.0	0.1	0.33	10	5	1.0
Na-depleting	0	5.4	101	17.9	6.0	0.1	0.33	10	5	0

The pH of the pipette solutions was adjusted to 7.15 with either 5 mM KOH (for 145 K/0 Na) or 4.5 mM NaOH plus 0.5 mM KOH (for 130 Na/15 K). The right-most two columns for pipette solutions give final concentrations of Na^+ and K^+. The pH of the extracellular solutions was adjusted to 7.40 with 5 mM NaOH (for Ca-free Tyrode's solution and Na-loading solution) or 130 mM HCl (for NMDG Tyrode's solution) or 97 mM HCl plus 1.3 mM NaOH (for Na-depleting solution). Final Na^+ concentrations were 140 mM (Ca-free Tyrodes's solution), 0.33 mM (NMDG Tyrode's solution), 106 mM (Na-loading solution), and 1.6 mM (Na-depleting solution). Note that all extracellular solutions shown here are essentially free of Ca^{2+}.

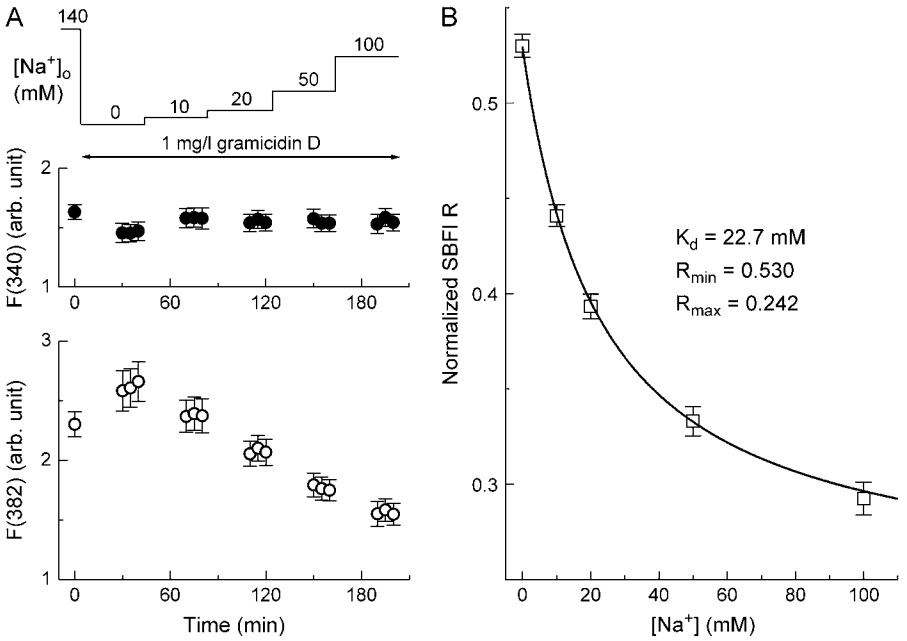

FIGURE 1 Intracellular calibration of SBFI fluorescence. (*A*) Fluorescence signals at 340-nm excitation (●) and 382 nm (○) were first measured in Ca-free Tyrode's solution and during the subsequent calibration runs in which extracellular Na^+ concentration was sequentially changed as indicated at the top (in mM) in the presence of 1 mg/l gramicidin D. Each data point represents mean ± SE of 13 cells. (*B*) The relationship between $[Na^+]$ and SBFI *R* (normalized to the standard *R*; during the course of these measurements, the normalization factor was 0.295) obtained in the calibration runs is shown in panel *A*. Data points are means ± SE of the 13 calibration runs. A solid line indicates the least-squares fit to the pooled data by a theoretical 1:1 binding curve (cf. Eq. 1) with parameters shown in the panel.

Against the latter possibility, gramicidin D likely permeabilizes the cell membrane, but not the membranes of intracellular organelles (19,20). In the following analysis, we therefore assumed that $[Na^+]_i$ (i.e., apparent cytoplasmic $[Na^+]$ measured in this study as the spatially averaged Na^+ concentration in the entire cell volume) closely reflected $[Na^+]_c$. Our estimates of $[Na^+]_i$ averaged ~12 mM in the Ca^{2+}-free Tyrode's solution (see below).

Perforated patch clamp

In some experiments, the perforated patch clamp was performed as described previously (16). Briefly, the glass pipette (resistance 4–6 MΩ when filled with the pipette solution) was first dipped into the pipette solution (Table 1), and then backfilled with the same solution containing 600 μg/ml amphotericin B. The pipette solution contained 145 mM monovalent cations ($[Na^+] + [K^+]$), 1 mM Ca^{2+}, and 1 mM Mg^{2+} (Table 1); Ca^{2+} was included to detect spontaneous rupture of the patch membrane. After a GΩ seal was formed, cell membrane perforation was monitored by observation of the capacitive currents in response to voltage pulses (±10 mV from the holding potential of −80 mV) delivered at 20 Hz from an Axopatch 200B amplifier (Axon Instruments, Foster City, CA). We generally started fluorescence measurements when the series resistance dropped to ≤30 MΩ. The series resistance during the period analyzed for the initial rate of decrease in $[Mg^{2+}]_i$ was, on average, 25.0 ± 1.6 MΩ (mean ± SE; $n = 18$). The average voltage error (calculated as the holding current times series resistance) was −5.4 ± 1.6 mV (range between −2.5 and −7.5 mV). Cell capacitance varied between 101 and 130 pF. All voltage data presented in this study have been corrected for a liquid junction potential of −10 mV, as liquid junction potentials between −8 and −12 mV were found between the pipette solution and various bath solutions (Table 1).

Solutions and experimental procedure

The extracellular solutions for superfusion of the myocytes were designed to maintain the K-Cl product ($[K^+] \times [Cl^-]$) and osmolality constant (Table 1). For observation of Mg^{2+} efflux, the myocytes were first loaded with Mg^{2+} by incubation in a solution of high Mg^{2+} concentration for ~3 h. The two solutions for Mg^{2+} loading both contained 24 mM Mg^{2+} (Na-loading solution and Na-depleting solution; Table 1) but different Na^+ concentrations. The Na-loading solution contained a relatively high Na^+ concentration (106 mM) plus 1 mM ouabain; the Na-depleting solution contained 1.6 mM Na^+, achieved by replacement of NaCl with NMDG-Cl (*N*-methyl-D-glucamine titrated by HCl). After $[Mg^{2+}]_i$ was significantly elevated above the resting level with concomitant Na^+ loading or Na^+ depletion, Mg^{2+} efflux was induced by changing the extracellular solution back to the standard Ca-free Tyrode's solution, which contained 1 mM Mg^{2+} and 140 mM Na^+ (Table 1). The initial rate of change in $[Mg^{2+}]_i$ (initial $\Delta[Mg^{2+}]_i/\Delta t$) was analyzed as an index of the rate of Mg^{2+} efflux. The initial $\Delta[Mg^{2+}]_i/\Delta t$ was estimated by linear regression of data points spanning 180 s (60–240 s after solution exchange; *solid lines* in Figs. 4, 5, 6, and 8). Because our previous work showed that the initial $\Delta[Mg^{2+}]_i/\Delta t$ values depend strongly on $[Mg^{2+}]_i$ levels, comparisons of the initial $\Delta[Mg^{2+}]_i/\Delta t$ values were made at comparable initial $[Mg^{2+}]_i$ (defined as $[Mg^{2+}]_i$ at the first point of the fitted line).

When the initial $\Delta[Mg^{2+}]_i/\Delta t$ was estimated at various $[Na^+]_o$, NaCl of the Ca-free Tyrode's solution was isosmotically replaced by NMDG-Cl. In practice, this was done by mixture of the Ca-free Tyrode's solution that contained 140 mM Na^+ and NMDG-Tyrode's solution that contained 0.33 mM Na^+ (Table 1) at the appropriate volume ratio.

Calculation of total cytoplasmic Mg concentration

To obtain quantitative information on Mg^{2+} flux across the cell membrane, we used the calculation method developed by Tursun et al. (8) to estimate total cytoplasmic Mg concentration ($[Mg_{tot}]$). Because, on average, 78% of furaptra molecules are localized in the cytoplasm with the rest being localized in organelles, the measured values of $[Mg^{2+}]_i$ were first corrected for $[Mg^{2+}]$ in the organelles to calculate $[Mg^{2+}]_c$, as previously described (8). Under the assumption that the fluorescence *R* measured in intact myocytes (R_i) could be expressed as the linear combination of *R* in the cytoplasm (R_c) and residual *R* in the organelles (R_r), the value of R_c could be calculated with the R_r value set to 0.8875, which corresponded to 0.65 mM $[Mg^{2+}]$ (the median value of the 0.6–0.7-mM range):

$$R_c = (R_i - 0.22 \times R_r)/0.78. \quad (2)$$

$[Mg^{2+}]_c$ was then calculated with Eq. 1 as described in Methods.

The model then utilized concentration and dissociation constant values for metals (Ca^{2+}, Mg^{2+}, Na^+, and K^+) of known cytoplasmic Mg^{2+}

buffers, as listed in Table 3 of Tursun et al. (8) to estimate the concentration of Mg-bound buffers by solving simultaneous equations. $[Mg_{tot}]$ values were calculated as the sum of bound Mg to each buffer site and $[Mg^{2+}]_c$. Traces of $[Mg_{tot}]$ thus obtained had very similar time courses to those of $[Mg^{2+}]_i$ with a larger ordinate scale (cf. Figs. 2 and 9 of Tursun et al. (8)). Values of initial $[Mg^{2+}]_c$ and the initial rate of change in $[Mg_{tot}]$ (initial $\Delta[Mg_{tot}]/\Delta t$) were obtained as described above for initial $[Mg^{2+}]_i$ and initial $\Delta[Mg^{2+}]_i/\Delta t$, and were used for analysis.

Data analysis

Cell membrane capacitance and series resistance were estimated with pCLAMP software (Clampex version 8.1.0.12; Axon Instruments). Fluorescence data were analyzed with the program Origin (version 7.0, OriginLab, Northampton, MA). Statistical values are expressed as the mean ± SE. Statistical significance was tested by Student's two-tailed *t*-test with the significance level set at $P < 0.05$.

RESULTS

Intracellular Na^+ loading

Basal $[Na^+]_i$ in 42 myocytes superfused with Ca^{2+}-free Tyrode's solution was estimated to be, on average, 11.8 ± 1.3 mM. Fig. 2 shows changes in $[Na^+]_i$ during Mg^{2+} loading with simultaneous Na^+ loading (*A*) and Na^+ depletion (*B*) of the myocytes. Incubation in the Na-loading solution (Table 1) caused a slow elevation of $[Na^+]_i$, which reached, on average, 31 mM in 1 h, and 47 mM in 3 h (Fig. 2 *A*). In contrast, the myocytes were quickly depleted of Na^+ within 30 min, and average $[Na^+]_i$ approached zero in 3 h in the Na^+-depleting solution (Fig. 2 *B*). The results confirm that these procedures for Na^+ loading and Na^+ depletion can effectively change $[Na^+]_i$ over a wide range (0–50 mM). Because we could not measure $[Na^+]_i$ and $[Mg^{2+}]_i$ simultaneously from the same cells, owing to the overlap of fluorescence spectra of SBFI and furaptra, $[Mg^{2+}]_i$ measurements were carried out under conditions of Na^+ loading or Na^+ depletion in separate sets of experiments.

Effects of Na^+ on fluorescence signals of furaptra

We previously found a small interference in furaptra fluorescence signals due to intracellular Na^+ (8). In that study, reduction of $[Na^+]_i$ from ~12 mM (see above) to much lower levels on removal of extracellular Na^+ caused a slight increase in furaptra *R*, which corresponded to an average reduction of 0.03–0.04 mM $[Mg^{2+}]_i$ when calibrated under the assumption that *R* signals exclusively reflect Mg^{2+} concentration. The change in *R* was reversed by reintroduction of 140 mM extracellular Na^+ (8). Because $[Na^+]_i$ was raised to much higher levels in this study (~50 mM; Fig. 2 *A*), we examined the effects of Na^+ on furaptra more extensively both in vitro and in vivo.

As shown in the top panel of Fig. 3 *A*, replacement of 150 mM KCl by 150 mM NaCl in salt solutions caused changes in the excitation fluorescence spectra of furaptra. The effect was somewhat greater in the absence than in the presence of Mg^{2+}. Difference spectra for Mg^{2+} (at 0 $[Na^+]$) and Na^+ (at 0 $[Mg^{2+}]$) are not dramatically different in their wavelength dependence, with isosbestic wavelengths at ~350 nm and maximum changes at ~380 nm (the *bottom* panel of Fig. 3 *A*), which makes it difficult to distinguish between Mg^{2+}-related and Na^+-related fluorescence changes at any wavelength. Fig. 3 *B* shows the results of fluorescence *R* measurements as a function of $[Mg^{2+}]$ carried out in the solutions containing various concentrations of Na^+. The plots show a clear $[Na^+]$-dependent displacement of the relation with a greater reduction of furaptra *R* at lower $[Mg^{2+}]$; 150 mM Na^+ caused a large reduction of R_{min} (by 0.103) with a slight increase in R_{max} (by 0.037) and essentially no change in K_D (see the fitted binding curve with *inverted triangles* in Fig. 3 *B*). When the curves for 10, 50, and 150 mM $[Na^+]$ are shifted rightward along the abscissa by 0.03, 0.15, and 0.53 mM, respectively, the shifted curves match the curve for 0 mM $[Na^+]$ (*inset* of Fig. 3 *B*), suggesting a parallel leftward shift of the relation in the presence of Na^+. Because Na^+ gives a constant offset to $[Mg^{2+}]$ values estimated from furaptra *R*, use of the calibration curve for 0 mM $[Na^+]$ will cause an overestimation of $[Mg^{2+}]$ by an error that is roughly proportional to $[Na^+]$.

Effects of Na^+ on the furaptra fluorescence signals were also examined in the myocytes (Fig. 4). After the cells were loaded with Mg^{2+} and Na^+ by incubation in the Na-loading

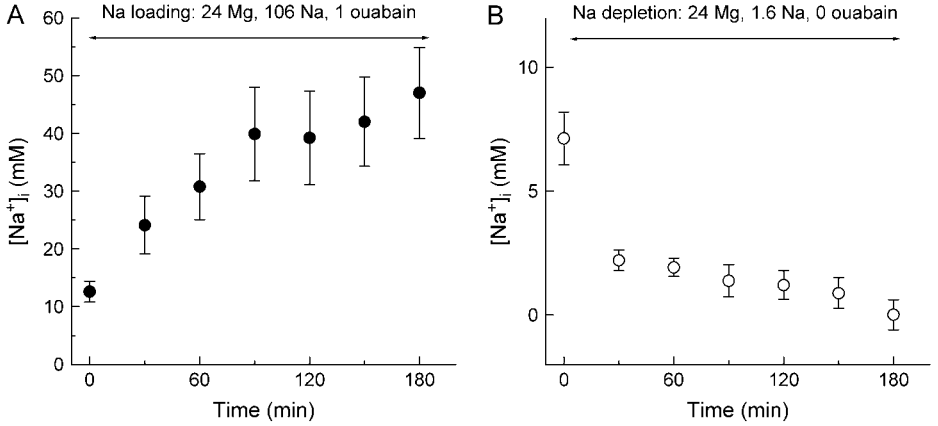

FIGURE 2 Changes in $[Na^+]_i$ during intracellular Mg^{2+} loading with either Na^+ loading (*A*) or Na^+ depletion (*B*). After the initial measurement of $[Na^+]_i$ in Ca-free Tyrode's solution at time 0, either the Na^+-loading solution or the Na^+-depleting solution was introduced (see Table 1), and the measurements were repeated as a function of time during a period of 3 h. Each symbol represents mean ± SE, $n = 21$ (*A*), 12 (*B*).

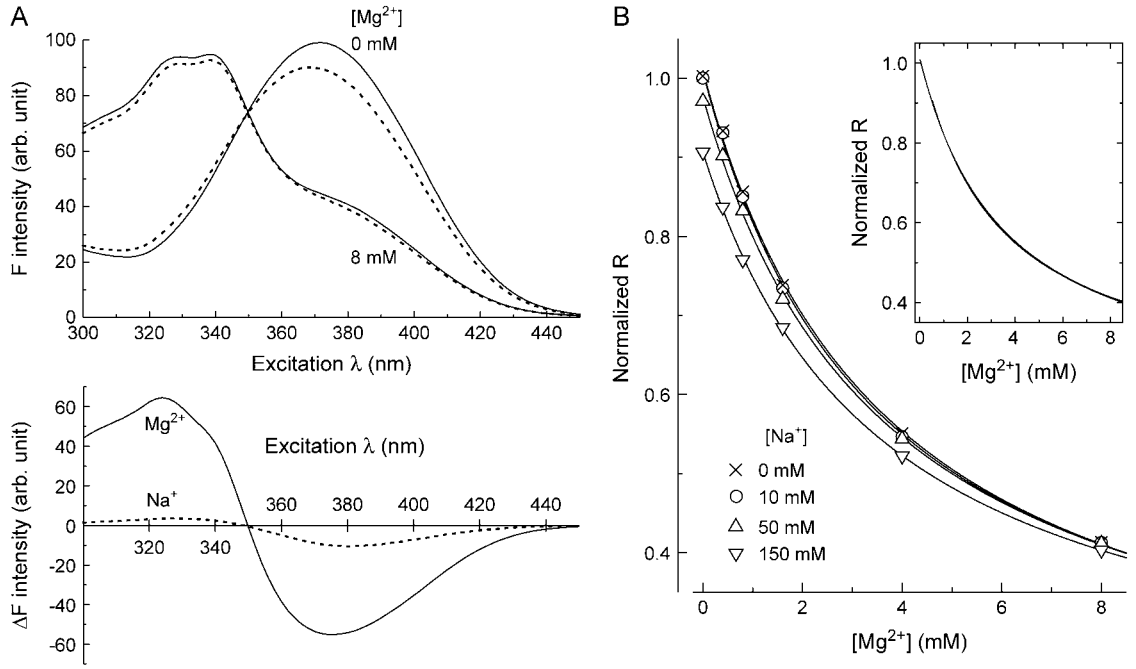

FIGURE 3 In vitro measurements of furaptra fluorescence in the solutions containing various concentrations of Na^+ and Mg^{2+} at 25°C. The solutions contain 150 mM NaCl plus KCl (Na^+ and K^+ were varied reciprocally), 1 mM K_2EGTA, 0–8.35 mM $MgCl_2$, and 5 mM HEPES (pH 7.15 by KOH). Free Mg^{2+} concentration was set by calculation with an apparent dissociation constant assumed for the Mg^{2+}-EGTA reaction: 14.9 mM at pH 7.15, ionic strength 0.16 M, and 25°C (37). (*A*) Fluorescence excitation spectra (*top*) and difference spectra (*bottom*) of 1 μM furaptra measured at 500 ± 10 nm (central wavelength ± half-width) in a 1-cm quartz cuvette with a spectrofluorometer (FP-6500; JASCO, Tokyo, Japan). In the top panel, solid lines and dashed lines were obtained, respectively, at 0 and 150 mM $[Na^+]$ with the free Mg^{2+} concentrations indicated near the curves. The bottom panel shows difference spectra for Mg^{2+} at 0 mM $[Na^+]$ (*solid line*) and for Na^+ at 0 mM $[Mg^{2+}]$ (*dashed line*) calculated from the spectra in the top panel. (*B*) Normalized fluorescence *R* (ordinate) of 50 μM furaptra measured as a function of $[Mg^{2+}]$ (abscissa). Quartz capillaries (i.d. ~ 50 μm) that contained the furaptra solution were placed in the superfusion bath used for the cell experiments. The solution contained 0 mM (×), 10 mM (○), 50 mM (△), or 150 mM (▽) Na^+. Each data point represents a mean value of 10 measurements. Solid lines were drawn by least-squares fitting to the data sets with Eq. 1. The fitted values for K_D, R_{min}, and R_{max} are, respectively; 3.65 mM, 1.010, and 0.138 for ×; 3.53 mM, 1.008, and 0.147 for ○; 3.68 mM, 0.978, and 0.149 for △; 3.62 mM, 0.907, and 0.175 for ▽.

solution (Table 1) for 3 h, NMDG Tyrode's solution that contained only 0.33 mM Na^+ (Table 1) was introduced. In contrast to the previous observation that $[Mg^{2+}]_i$ of the Mg^{2+}-loaded (but not Na^+-loaded) myocytes stayed constant upon introduction of a solution that was essentially free of Na^+ ((16); also note the average initial $\Delta[Mg^{2+}]_i/\Delta t$ value of −0.02 μM/s in Table 2), $[Mg^{2+}]_i$ (apparent $[Mg^{2+}]_c$) decreased substantially and reached a new quasisteady level within 10 min (Fig. 4, *top panel*). The different results obtained with or without intracellular Na^+ loading strongly suggest that the decrease in $[Mg^{2+}]_i$ observed in this study is due to a decrease in $[Na^+]_c$ rather than $[Mg^{2+}]_c$, because: 1), the in vitro measurements (Fig. 3) indicate that a decrease in either $[Mg^{2+}]$ or $[Na^+]$ caused an increase in furaptra *R*; 2), it has been reported that $[Na^+]_c$ quickly decreases upon removal of extracellular Na^+ (21); and 3), the myocytes were likely depleted of Na^+ after 10-min superfusion with the NMDG Tyrode's solution, as the subsequent introduction of 140 mM Na^+ caused a quick reduction of $[Mg^{2+}]_i$ with an initial $\Delta[Mg^{2+}]_i/\Delta t$ similar to those observed in the Na^+-depleted cells (*top panel* of Fig. 4; see also Fig. 7).

The bottom panel of Fig. 4 shows the results of experiments carried out in eight myocytes with the protocol shown in the top panel of Fig. 4. The relation between $[Mg^{2+}]_i$ after intracellular loading of Na^+ (and Mg^{2+}) and the change in $[Mg^{2+}]_i$ during Na^+ unloading for 10 min ($\Delta[Mg^{2+}]_i$) showed little dependence of $\Delta[Mg^{2+}]_i$ on $[Mg^{2+}]_i$ with a mean $\Delta[Mg^{2+}]_i$ of −0.12 ± 0.008 mM (Fig. 4, *bottom panel*). Because $[Na^+]_i$ after the Na^+ loading for 3 h was, on average, 47 mM (Fig. 2 *A*), the offset value of $[Mg^{2+}]_i$ that is attributable to $[Na^+]_i$, 0.12 mM, may be compared to the value found in the solution that contained 50 mM Na^+, 0.15 mM (Fig. 3 *B*). Thus, the Na^+-related offsets estimated in vivo and in vitro were similar and were independent of $[Mg^{2+}]$. In the following analysis of the cells loaded with Na^+ for 3 h (e.g., Fig. 5 *A*), we therefore subtracted the constant value of 0.12 mM from each data point of the $[Mg^{2+}]_i$ traces calibrated from furaptra *R*; this empirical correction reduced the initial $[Mg^{2+}]_i$ values by 0.12 mM with no change in the values of initial $\Delta[Mg^{2+}]_i/\Delta t$. For the experiments of Na^+ loading for 1 h (average $[Na^+]_i$ ~ 31 mM), a modified correction was used. We assumed that the offset was proportional to $[Na^+]_i$, as observed in vitro (Fig. 3), and the value of 0.08 mM (=0.12 mM × 31 / 47) was subtracted from each data point.

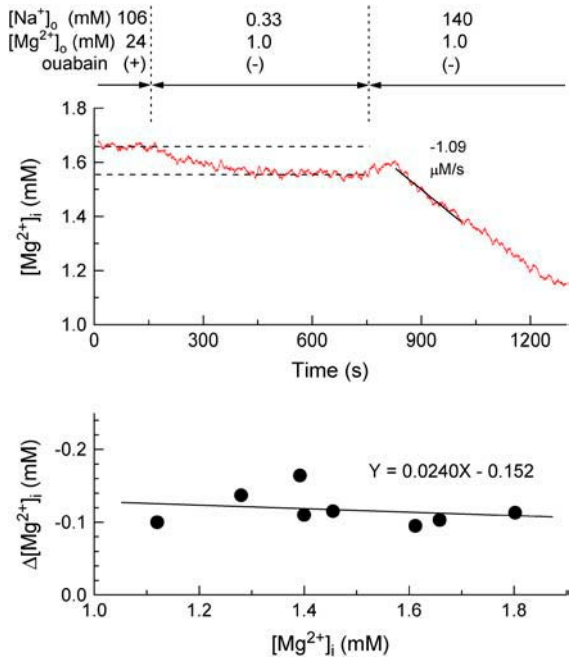

FIGURE 4 Effects of $[Na^+]_i$ on the $[Mg^{2+}]_i$ measurement with furaptra. (*Top*) A record of the run obtained from a myocyte. The cell was loaded with Mg^{2+} and Na^+ by incubation in the Na^+-loading solution for 3 h, and then intracellular Na^+ was unloaded by perfusion with NMDG Tyrode's solution that contained only 0.33 mM Na^+ and no ouabain, as indicated. At the end of the 10-min perfusion with the NMDG Tyrode's solution, Ca-free Tyrode's solution was introduced as indicated. Values of $[Mg^{2+}]_i$ (ordinate) were calculated from the fluorescence R under the assumption of no interference by $[Na^+]_i$. Note that reduction of extracellular Na^+ caused a slow decrease in $[Mg^{2+}]_i$, and the subsequent introduction of 140 mM Na^+ induced a rapid decrease in $[Mg^{2+}]_i$. In this figure and subsequent figures, a solid line was drawn by the linear least-squares fit to data points for 180 s, and the initial $\Delta[Mg^{2+}]_i/\Delta t$ estimated from the slope is indicated (μM/s) near the trace. Cell 060403. (*Bottom*) The change in $[Mg^{2+}]_i$ ($\Delta[Mg^{2+}]_i$) was defined as the difference between the $[Mg^{2+}]_i$ levels at the beginning and at the end of the 10-min perfusion by NMDG Tyrode's solution, as shown by the dashed lines in the top panel. Values of $\Delta[Mg^{2+}]_i$ obtained from eight myocytes are plotted as a function of the $[Mg^{2+}]_i$ level at the beginning of the perfusion with NMDG Tyrode's solution (●). The solid line indicates the linear regression for the data points of the form indicated in the panel.

Relation between $[Na^+]_i$ and the rate of Mg^{2+} efflux

Fig. 5 shows examples of the initial $\Delta[Mg^{2+}]_i/\Delta t$ measurement for cells that were loaded with Mg^{2+} to similar $[Mg^{2+}]_i$ levels (~1.5 mM). The extracellular Na^+-related Mg^{2+} efflux was slower in the myocyte loaded with Na^+ for 3 h (Fig. 5 *A*) than in the myocyte depleted of Na^+ for 3 h (Fig. 5 *B*). For the Na^+-loaded myocytes, 1 mM ouabain was present not only during the Na^+ (and Mg^{2+}) loading, but throughout the $[Mg^{2+}]_i$ measurement runs. However, ouabain is unlikely to have a direct effect on the Mg^{2+} transport, because application of ouabain only during the time of Mg^{2+} efflux for a Na^+-depleted cell had little influence on the initial $\Delta[Mg^{2+}]_i/\Delta t$ (Fig. 5 *C*). Results obtained from the cells having repeated measurements are summarized in Table 2. When the myocytes were loaded with Na^+ for 3 h (average $[Na^+]_i \sim 47$ mM), the average initial $\Delta[Mg^{2+}]_i/\Delta t$ was estimated to be -0.43 ± 0.16 μM/s. This value is ~40% of that for the Na^+-depleted cells (-1.09 ± 0.11 μM/s) at comparable initial $[Mg^{2+}]_i$ (1.45 ± 0.11 and 1.47 ± 0.11 mM; Table 2).

We also examined the effect of intermediate $[Na^+]_i$ by loading the cells with Na^+ only for 1 h (average $[Na^+]_i \sim 31$ mM). The initial $\Delta[Mg^{2+}]_i/\Delta t$ was comparable to that obtained after Na^+ loading for 3 h at much lower initial $[Mg^{2+}]_i$ levels (1.18 ± 0.07 mM; Table 2). When the cells were loaded with Na^+ for 3 h and then unloaded for 10 min in the essential absence of extracellular Na^+ (Fig. 4), the initial $\Delta[Mg^{2+}]_i/\Delta t$ was comparable to that for the cells depleted of Na^+ (without Na^+ loading) at comparable initial $[Mg^{2+}]_i$ levels.

Manipulation of $[Na^+]_i$ with patch-pipette loading

In some experiments, $[Na^+]_i$ was directly manipulated by intracellular perfusion from the patch pipette. The myocytes were loaded with Mg^{2+} in the Na-depleting solution (Table 1) for 3–5 h, and then exposed to pipette solution containing either 130 mM Na^+ plus 15 mM K^+ (130 Na/15 K) or zero Na^+ plus 145 mM K^+ (145 K/0 Na). Although we did not estimate $[Na^+]_i$ in these conditions, $[Na^+]_i$ of the myocytes internally perfused with the 145 K/0 Na solution was very likely close to zero, whereas $[Na^+]_i$ was probably elevated to higher levels by internal perfusion with the 130 Na/15 K solution. It is unlikely at low $[Na^+]_o$ (the Na-depleting solution), however, that perfusion through the perforated cell membrane was effective enough to equalize $[Na^+]_i$ with the pipette Na^+ concentration. We found that the extracellular Na^+-dependent Mg^{2+} efflux was slower with the pipette of high Na^+ concentration (130 Na/15 K solution), when compared with the myocytes loaded with Mg^{2+} to similar levels (Fig. 6). (Note that we did not have any estimate of the Na^+-related offset for the myocytes internally perfused with the 130 Na/15 K solution. Because the initial $\Delta[Mg^{2+}]_i/\Delta t$ values in these myocytes were similar to those observed in the cells loaded with Na^+ for 3 h (Table 2), we somewhat arbitrarily assumed the same offset (0.12 mM) as that used for the Na^+-loaded myocytes. No subtraction of the Na^+-related offset was applied for data obtained with the 145 K/0 Na pipette solution.)

Summary of $[Na^+]_i$ dependence

Table 2 compares the values of initial $[Mg^{2+}]_i$ and initial $\Delta[Mg^{2+}]_i/\Delta t$ obtained in various experimental conditions. For the patch-clamp experiments, data taken from Tashiro et al. (16) were also included. It is clear that the initial $\Delta[Mg^{2+}]_i/\Delta t$ was little influenced by 10 mM pipette Na^+ ($[Na^+]_p$), but was markedly reduced by 130 mM $[Na^+]_p$ at the same $[Na^+]_o$.

Because Mg^{2+} is buffered in the cytoplasm, the rate of changes in $[Mg_{tot}]$ ($\Delta[Mg_{tot}]/\Delta t$) would be more directly

TABLE 2 Analysis of the initial rate of decrease in $[Mg^{2+}]_i$ at 25°C

Experimental conditions	*n*	Initial $[Mg^{2+}]_i$	Initial $\Delta[Mg^{2+}]_i/\Delta t$	Initial $[Mg^{2+}]_c$	Initial $\Delta[Mg_{tot}]/\Delta t$ $\Delta[Mg^{2+}]_i/\Delta t$
		mM	μM/s	mM	μM/s
Extracellular $[Na^+]$*					
140 mM	10	1.47 ± 0.109	−1.09 ± 0.105	1.75 ± 0.152	−2.40 ± 0.197
70 mM	7	1.47 ± 0.022	−0.84 ± 0.085	1.74 ± 0.031	−1.82 ± 0.185
42 mM	6	1.47 ± 0.079	−0.51 ± 0.031	1.74 ± 0.110	−1.11 ± 0.077
21 mM	6	1.44 ± 0.045	−0.22 ± 0.037	1.70 ± 0.062	−0.48 ± 0.078
Ouabain†					
1 mM	3	1.48 ± 0.180	−1.17 ± 0.230	1.76 ± 0.251	−2.62 ± 0.535
Na-loading‡					
1 h	6	1.18 ± 0.068	−0.52 ± 0.087	1.34 ± 0.097	−1.22 ± 0.198
3 h	8	1.45 ± 0.107	−0.43 ± 0.161	1.72 ± 0.149	−0.95 ± 0.342
Na-loading + unloading§					
3 h + 10 min	8	1.35 ± 0.089	−0.99 ± 0.103	1.59 ± 0.122	−2.21 ± 0.188
Patch-clamp experiments¶					
$[Na^+]_p$ / $[Na^+]_o$					
0 mM / 140 mM	4	1.58 ± 0.159	−1.21 ± 0.177	1.90 ± 0.223	−2.62 ± 0.364
10 mM / 140 mM‖	9	1.47 ± 0.117	−1.18 ± 0.228	1.75 ± 0.162	−2.56 ± 0.457
130 mM / 140 mM	4	1.31 ± 0.120	−0.41 ± 0.061	1.52 ± 0.164	−0.93 ± 0.115
10 mM / 70 mM‖	13	1.58 ± 0.083	−0.79 ± 0.092	1.91 ± 0.116	−1.68 ± 0.183
10 mM / 0 mM‖	16	1.56 ± 0.063	−0.02 ± 0.039	1.87 ± 0.088	−0.04 ± 0.082

Columns contain mean ± SE values of initial $[Mg^{2+}]_i$ (column 3), initial $\Delta[Mg^{2+}]_i/\Delta t$ (column 4), initial $[Mg^{2+}]_c$ (column 5) and initial $\Delta[Mg_{tot}]/\Delta t$ (the rightmost column) from *n* cells (column 2) in each experimental condition (the leftmost column). For the statistics, we included data only from the cells that were moderately loaded with Mg^{2+} (i.e., initial $[Mg^{2+}]_i$ between 1.0 and 2.0 mM). To convert values of $\Delta[Mg_{tot}]/\Delta t$ (in μM/s) to Mg^{2+} flux (in pmol/cm^2 s or pmol/μF s), the initial $\Delta[Mg_{tot}]/\Delta t$ values should be multiplied by 0.08 (see text for details).

*Na^+-depleted cells (cf. Figs. 2 *B* and 5 *B*).

†Cells were depleted of Na^+, and 1 mM ouabain was applied only during the initial $\Delta[Mg^{2+}]_i/\Delta t$ measurements at 140 mM $[Na^+]_o$ (cf. Figs. 2 *B* and 5 *C*).

‡Cells were loaded with Na^+ for 1 or 3 h, and the initial $\Delta[Mg^{2+}]_i/\Delta t$ was measured at 140 mM $[Na^+]_o$ (cf. Figs. 2 *A* and 5 *A*).

§Cells were initially loaded with Na^+ for 3 h, and then were unloaded by incubation in the essentially Na^+-free solution for 10 min before the $\Delta[Mg^{2+}]_i/\Delta t$ measurements at 140 mM $[Na^+]_o$ (cf. Figs. 2 *A* and 4).

¶Holding potential was −80 mV during the initial $\Delta[Mg^{2+}]_i/\Delta t$ measurements with the indicated pipette Na^+ concentration ($[Na^+]_p$) and $[Na^+]_o$.

‖Data taken from Tashiro et al. (16).

related to Mg^{2+} flux across the cell membrane. Based on the measured $[Mg^{2+}]_i$ values, we used the calculation method developed by Tursun et al. (8) to estimate $[Mg_{tot}]$, as described in Methods. Cytoplasmic concentrations of Na^+ ($[Na^+]_c$) and K^+ ($[K^+]_c$) were assumed to be 10 and 140 mM, respectively, except for data obtained from the Na^+-loaded myocytes; $[Na^+]_c$ was set to 31 mM (plus 119 mM $[K^+]_c$) and 47 mM (plus 103 mM $[K^+]_c$) for the myocytes loaded with Na^+ for 1 and 3 h, respectively (Fig. 2 *A*). $[Na^+]_c$ of 47 mM was also assumed for the myocytes patch-clamped with the 130 Na/15 K pipette solution. $[Ca^{2+}]_c$ was assumed to be 10 nM for the cells incubated in extracellular Ca^{2+}-free conditions (8). The values of initial $[Mg^{2+}]_c$ and initial $\Delta[Mg_{tot}]/\Delta t$ thus obtained are also summarized in Table 2.

For a more precise comparison, the initial $\Delta[Mg_{tot}]/\Delta t$ values were adjusted for variations in initial $[Mg^{2+}]_c$. For this purpose, we used the relation between the initial $[Mg^{2+}]_c$ and the initial $\Delta[Mg_{tot}]/\Delta t$ constructed previously (*solid curve* in Fig. 9 of Tursun et al. (8)) as a standard curve; any value of the initial $\Delta[Mg_{tot}]/\Delta t$ was normalized to the standard value on the curve at a given initial $[Mg^{2+}]_c$ to yield relative $\Delta[Mg_{tot}]/\Delta t$. Relative $\Delta[Mg_{tot}]/\Delta t$ values thus obtained with altered $[Na^+]_i$ are summarized in Fig. 7. In conditions where $[Na^+]_i$ was kept low, the relative $\Delta[Mg_{tot}]/\Delta t$ values were close to unity (columns *a–c*, *f*, and *g*), independent of the presence of ouabain (column *b*), history of Na^+ loading (column *c*), and intracellular perfusion with the pipette solution that contained 0–10 mM Na^+ (columns *f* and *g*). Intracellular Na^+ loading caused a significant reduction of the relative $\Delta[Mg_{tot}]/\Delta t$; the relative $\Delta[Mg_{tot}]/\Delta t$ decreased, on average, by 40.5 ± 9.8% after Na^+ loading for 1 h (when the average $[Na^+]_i$ was 31 mM), and by 63.6 ± 12.5% after Na^+ loading for 3 h (when the average $[Na^+]_i$ was 47 mM). Thus, $[Na^+]_i$ for 50% inhibition appears to lie halfway between 31 and 47 mM, and may be roughly ~40 mM. The relative $\Delta[Mg_{tot}]/\Delta t$ was significantly reduced with the high Na^+ concentration pipette (130 mM), which is in qualitative agreement with the results of the Na^+ loading/depletion experiments.

$[Na^+]_o$ dependence of the rate of Mg^{2+} efflux

Fig. 8 *A* shows the initial $\Delta[Mg^{2+}]_i/\Delta t$ measurements at different $[Na^+]_o$. After the myocytes were loaded with Mg^{2+}

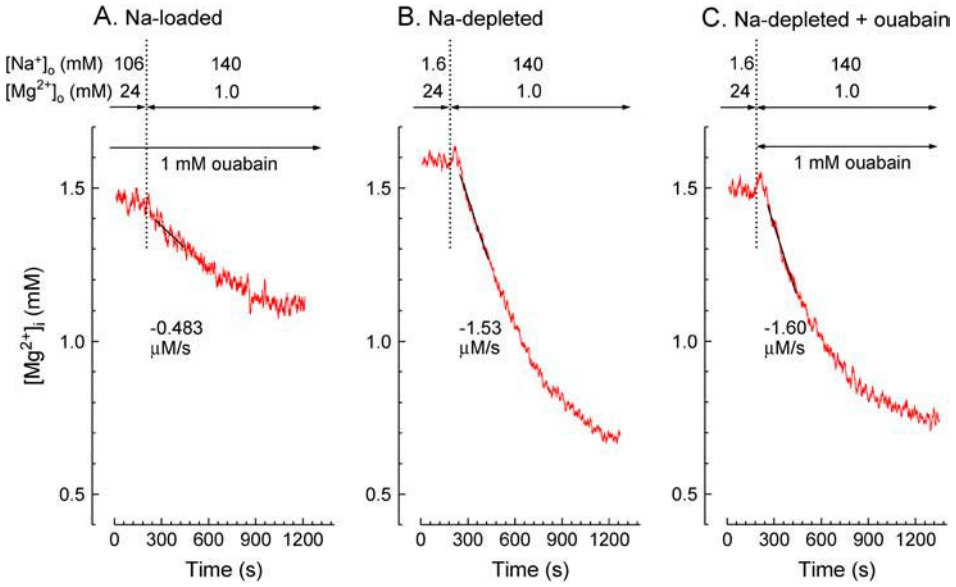

FIGURE 5 Extracellular Na^+-induced changes in $[Mg^{2+}]_i$ in the Mg^{2+}-loaded cells. Panels show records from three separate experiments in which extracellular concentrations of Na^+ and Mg^{2+} were changed as indicated above at the times shown by vertical dotted lines. Ouabain was also applied for the period as indicated. After cells were loaded with Mg^{2+} with either Na^+ loading (*A*) or Na^+ depletion (*B*, *C*), the perfusate was changed to Ca-free Tyrode's solution either in the presence (*A*, *C*) or absence of ouabain. Cells 080102 (*A*), 072502 (*B*), and 083002 (*C*). Estimated values of initial $\Delta[Mg^{2+}]_i/\Delta t$ are indicated (μM/s) near the traces.

in the Na-depleting solution (Table 1) for 3 h to reach 1.4–1.5 mM $[Mg^{2+}]_i$, the solution of 21, 42, or 70 mM $[Na^+]_o$ was applied to induce Mg^{2+} efflux. Note that the Mg^{2+} efflux was slower at lower $[Na^+]_o$. For the sets of experiments at 21, 42, 70, and 140 mM $[Na^+]_o$, the average initial $\Delta[Mg^{2+}]_i/\Delta t$ varied approximately from -0.2 to -1.1 μM/s at similar initial $[Mg^{2+}]_i$ levels (Table 2). For more complete analysis of the extracellular Na^+ dependence, we calculated the relative $\Delta[Mg_{tot}]/\Delta t$ using the standard relation between the initial $[Mg^{2+}]_c$ and the initial $\Delta[Mg_{tot}]/\Delta t$, as described above. The relative $\Delta[Mg_{tot}]/\Delta t$ data points were well fitted with a Hill curve with half-maximal activation at 55 mM $[Na^+]_o$. (Fig. 8 *B*). Fig. 8 *B* also includes data points obtained with the patch clamp at a holding potential of -80 mV (16). The lack of a significant difference between data obtained with or without the patch clamp suggests that a slight fluctuation of membrane potential, if any, little influences the rate of Mg^{2+} efflux. It has been reported that a change in membrane potential between -40 and -80 mV does not significantly change the initial $\Delta[Mg^{2+}]_i/\Delta t$ (16).

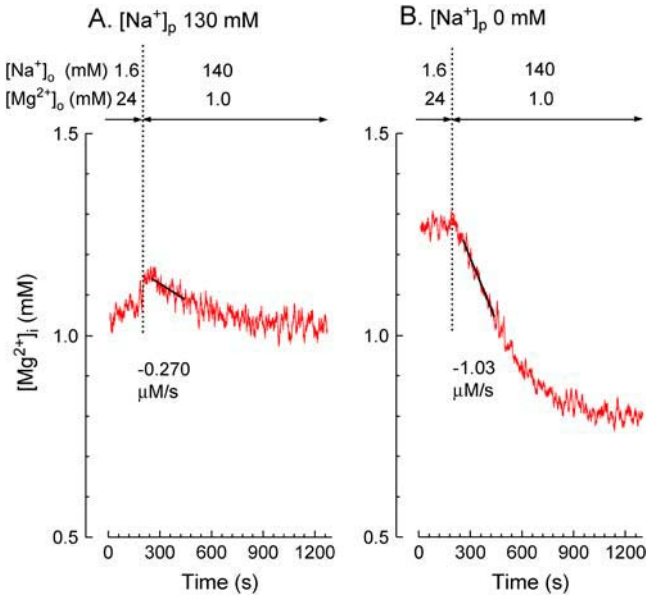

FIGURE 6 Extracellular Na^+-induced changes in $[Mg^{2+}]_i$ in the myocytes voltage-clamped at a holding potential of -80 mV using the perforated patch-clamp technique. Panels *A* and *B* show records from two separate experiments in which different pipette solutions were employed: 130 mM Na^+ plus 15 mM K^+ (*A*) and 0 mM Na^+ plus 145 mM K^+ (*B*). Extracellular Na^+ and Mg^{2+} concentrations were changed as indicated above at the times shown by vertical dotted lines. (*A*) Cell 092702-2, cell capacitance 105 pF, series resistance 27.2 MΩ; (*B*) cell 100402, cell capacitance 123 pF, series resistance 23.4 MΩ. The initial $\Delta[Mg^{2+}]_i/\Delta t$ estimated from the slope of the solid line is indicated (μM/s) near each trace.

Changes in $[Mg^{2+}]_i$ upon reversal of Na^+ gradient

In our previous studies (8,11,16), reversal of Na^+ gradient by removal of extracellular Na^+ failed to induce any detectable increase in $[Mg^{2+}]_i$, providing no evidence for the reversal of the Mg^{2+} transport (i.e., Mg^{2+} influx under reversed Na^+ gradient). In a new attempt to detect a possible Mg^{2+} influx (as an increase in $[Mg^{2+}]_i$), we heavily loaded cells with Na^+ by application of 1 mM ouabain in the presence of 140 mM extracellular Na^+ (Ca-free Tyrode's solution; Table 1), in combination with intracellular perfusion from the patch pipette that contained the solution of high $[Na^+]_p$ (130 Na/15 K solution; Table 1). Because the Na^+-related offsets for the $[Mg^{2+}]_i$ measurements are unknown in these experiments, we analyzed only the changes in $[Mg^{2+}]_i$ from the baseline (rather than levels of $[Mg^{2+}]_i$); note that the constant pedestal of $[Mg^{2+}]_i$ at any given $[Na^+]_i$ should not affect the estimates of the amplitude and the initial rate of $[Mg^{2+}]_i$ changes.

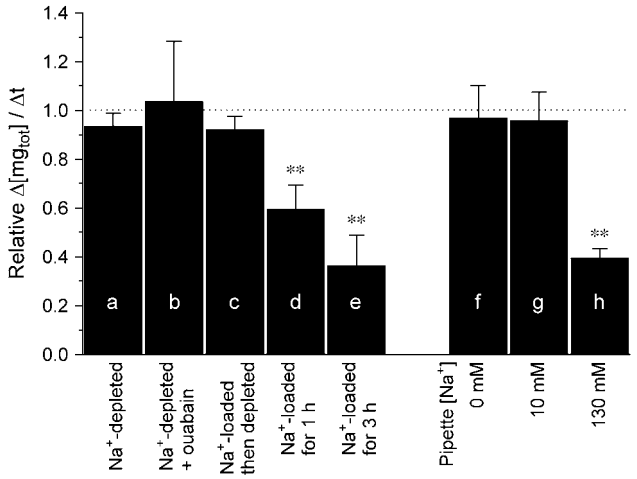

FIGURE 7 Summary of initial rates of decrease in $[Mg_{tot}]$ (initial $\Delta[Mg_{tot}]/\Delta t$) measured at 140 mM $[Na^+]_o$. All values of initial $\Delta[Mg_{tot}]/\Delta t$ were normalized to those expected for the initial $[Mg^{2+}]_c$ to calculate relative $\Delta[Mg_{tot}]/\Delta t$ (see text for details). Columns show means ± SE for data obtained without patch-clamp recordings (*a–e*) or under patch clamp with the holding potential of −80 mV (*f–h*). (*a*) Cells were depleted of Na^+ for 3 h in the Na-depleting solution (cf. Figs. 2 *B* and 5 *B*). (*b*) Cells were depleted of Na^+ for 3 h, and 1 mM ouabain was applied only after the Mg^{2+} efflux was induced (cf. Figs. 2 *B* and 5 *C*). (*c*) Cells were loaded with Na^+ for 3 h in the Na-loading solution, and then were unloaded by incubation in the essentially Na^+-free solution for 10 min (cf. Figs. 2 *A* and 4). (*d* and *e*) Cells were loaded with Na^+ for 1 and 3 h, respectively, in the Na-loading solution (Figs. 2 *A* and 5 *A*). (*f–h*) Na^+-depleted cells were patch-clamped at the holding potential of −80 mV with the pipette containing 0 mM (*f*), 10 mM (*g*), or 130 mM (*h*) Na^+ (cf. Fig. 6). See Table 2 for the number of cells. **, significantly different from 1.0 ($P < 0.01$).

After the membrane perforation was established as a drop in series resistance to ~25 MΩ (see Methods), the holding potential was changed to +20 mV (Fig. 9). A holding potential more positive than the equilibrium potential for Mg^{2+} (~0 mV under a very small concentration gradient of Mg^{2+} across the cell membrane) should passively drive Mg^{2+} outward; thus any influx of Mg^{2+} must be carried by an energy-linked transport. Reversal of the Na^+ gradient by superfusion of the Na^+-loaded myocytes with the essentially Na^+-free solution caused a slow increase in $[Mg^{2+}]_i$ (Fig. 9 *A*) with the average rate of +0.25 ± 0.070 μM/s ($n = 6$). When myocytes were internally perfused with a pipette solution containing no Na^+ (145 K/0 Na solution; Table 1), removal of extracellular Na^+ caused a decrease in $[Mg^{2+}]_i$ (Fig. 9 *B*), at an average rate of −0.23 ± 0.030 μM/s ($n = 4$). Thus, a rise of $[Mg^{2+}]_i$ was only observed under the condition of a large outward gradient of $[Na^+]$ across the cell membrane.

DISCUSSION

According to the Na^+-Mg^{2+} exchange hypothesis, Mg^{2+} extrusion from the cells should be favored by high $[Na^+]_o$ and high $[Mg^{2+}]_c$, and inhibited by an elevation in $[Na^+]_c$ and $[Mg^{2+}]_o$. Our previous study showed that a slight elevation of $[Mg^{2+}]_c$ strongly stimulates Mg^{2+} efflux in rat ventricular myocytes with half-maximal activation at 1.9 mM $[Mg^{2+}]_c$. Conversely, $[Mg^{2+}]_o$ inhibited the Mg^{2+} efflux with 50% inhibition at 10 mM (8). This study extends over the previous findings and further characterizes the Mg^{2+} transport. We found that the Mg^{2+} efflux is inhibited by intracellular Na^+ with 50% inhibition at ~40 mM $[Na^+]_c$, whereas it is stimulated in a concentration-dependent manner by extracellular Na^+, with half-maximal activation at 55 mM $[Na^+]_o$. All these findings fit within expectations for Na^+-Mg^{2+} exchange and provide important quantitative information on the interaction between Na^+ and Mg^{2+} on the transporter, which will be useful for constructing thermodynamic models of this transport system.

Optical measurements of $[Na^+]_i$ and $[Mg^{2+}]_i$

The cytoplasmic concentrations of Na^+ and Mg^{2+} were estimated with SBFI and furaptra, respectively. We used furaptra for Mg^{2+}, because its fluorescence *R* signals could be reliably calibrated in terms of $[Mg^{2+}]_c$ with parameters previously obtained in rat ventricular myocytes (17) including corrections for indicator molecules compartmentalized in intracellular organelles (8). SBFI was used for Na^+, because it is the only ratiometric Na^+ indicator commercially available; SBFI *R* could be converted to $[Na^+]_c$ with parameters estimated in the myocytes (Fig. 1). The use of ratiometric indicators is also important for monitoring $[Na^+]_c$ in conditions in which cell volume may be altered by significant changes in intracellular and extracellular ionic compositions. Unfortunately, it was not possible to separate fluorescence signals of furaptra and SBFI measured simultaneously from the same cell, due to the overlap of their fluorescence spectra.

We assumed that $[Na^+]_i$ calibrated from SBFI fluorescence signals was approximately equal to $[Na^+]_c$, as the intracellular calibration curve was obtained from the cells treated with gramicidin D, which selectively permeabilizes the cell membrane for small monovalent cations (18). The distribution of intracellular Na^+ and the relative contribution of SBFI fluorescence signals from the cytoplasm and intracellular organelles are expected to be maintained during the calibration run as in intact cells.

On the other hand, the intracellular calibration curve for furaptra was obtained in the presence of the ionophore mixture, under the condition in which Mg^{2+} distribution was thought to be uniform in the cells (17). Consequently, $[Mg^{2+}]_i$ calibrated from furaptra *R* likely underestimates $[Mg^{2+}]_c$ with an error that becomes progressively greater at higher $[Mg^{2+}]_c$. The measured $[Mg^{2+}]_i$ values were therefore corrected for $[Mg^{2+}]$ in the organelles as described in Methods. It should be noted that $[Mg^{2+}]$ in the intracellular organelles may not be significantly changed by elevation of $[Na^+]_c$. This is because, in the previous study (8), $[Mg^{2+}]$ in the intracellular organelles (primarily mitochondria) calibrated from furaptra *R* was ~0.8 mM at 50 mM $[Na^+]_c$.

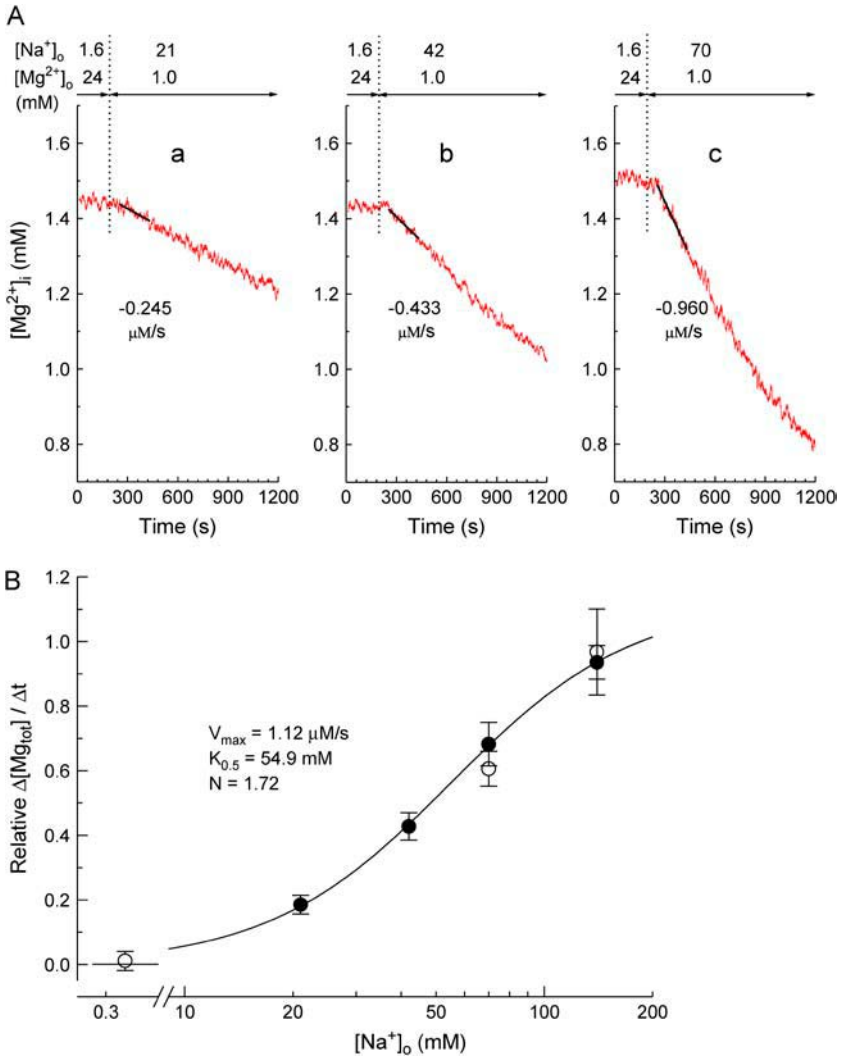

FIGURE 8 Extracellular Na^+ dependence of the initial rate of decrease in $[Mg^{2+}]_i$ (initial $\Delta[Mg^{2+}]_i/\Delta t$). (*A*) Records from three separate experiments in which the Mg^{2+} efflux was induced by 21 mM (*a*), 42 mM (*b*), or 70 mM (*c*) extracellular Na^+, as indicated above. The initial $\Delta[Mg^{2+}]_i/\Delta t$ estimated from the slope of a solid line is indicated below each trace. Cells 100103 (*a*), 091803 (*b*), and 080803 (*c*). (*B*) Solid circles show the relation between $[Na^+]_o$ and relative $\Delta[Mg_{tot}]/\Delta t$ obtained from the type of experiments shown in panel *A*. Open circles were obtained from the perforated patch-clamp experiments with 10 mM $[Na^+]_p$ and the holding potential of −80 mV (taken from Tashiro et al. (16)). Each symbol represents mean ± SE from 6 to 16 cells (see Table 2 for the number of cells). A solid line indicates least-squares fit of the accumulated data (●) by the Hill curve with parameters shown in the panel: relative $\Delta[Mg_{tot}]/\Delta t = V_{max} \times [Na^+]_o^N / (K_{0.5}^N + [Na^+]_o^N)$, where V_{max} denotes the maximum value of relative $\Delta[Mg_{tot}]/\Delta t$, N is the Hill coefficient, and $K_{0.5}$ is $[Na^+]_o$ that gives half-maximal value of relative $\Delta[Mg_{tot}]/\Delta t$.

When this value was adjusted for the Na^+-related offset (0.12 mM), the corrected $[Mg^{2+}]$ was ~0.68 mM. This is within the 0.6–0.7-mM range found in the organelles at 0–10 mM $[Na^+]_c$ (8), with no evidence of alteration in $[Mg^{2+}]$ in the organelles by elevation of $[Na^+]_c$ up to 50 mM. It is also noteworthy that variations of Na^+, K^+, and Ca^{2+} concentrations do not markedly change the cytoplasmic Mg^{2+} buffering power (defined as $d[Mg_{tot}]/d[Mg^{2+}]_c$), according to our model (8). For example, the buffering power at 0.9 mM $[Mg^{2+}]_c$ increased by only 1.3% by the elevation of $[Na^+]_c$ from 10 to 50 mM (with a concomitant decrease in $[K^+]_c$ from 140 to 100 mM). Thus, these data obtained from furaptra fluorescence (initial $\Delta[Mg^{2+}]_i/\Delta t$ and initial $\Delta[Mg_{tot}]/\Delta t$) likely provide valid information on the rate of Mg^{2+} flux.

Dependence of Mg^{2+} efflux on intracellular and extracellular Na^+ concentrations

The results summarized in Fig. 7 clearly show that elevation of $[Na^+]_c$ inhibits the rate of Mg^{2+} efflux in rat ventricular myocytes. Using rat erythrocytes, Günther et al. (22) studied the dependence of Mg^{2+} efflux on total [Na] ($[Na_{tot}]$) measured with atomic absorption spectroscopy, and reported that Mg^{2+} efflux was inhibited competitively by intracellular Na^+, with 50% inhibition at 15 mM cellular $[Na_{tot}]$. Handy et al. (10) measured $[Mg^{2+}]_i$ of rat ventricular myocytes using furaptra, and found that application of strophanthidin caused an increase in $[Mg^{2+}]_i$, which could be interpreted as an increased Mg^{2+} influx (or inhibited Mg^{2+} efflux) at elevated $[Na^+]_c$. In that study, however, $[Na^+]_c$ was not estimated, and the effects of $[Na^+]_c$ on the Mg^{2+} efflux were not quantitatively analyzed. The 50% inhibition at ~40 mM $[Na^+]_c$ found in this study suggests that the rate of Mg^{2+} extrusion transport is reduced by elevation of $[Na^+]_c$ only to levels well above the basal level (~12 mM). In contrast, lowering $[Na^+]_c$ from the basal level by intracellular perfusion with the Na^+-free (145 K/0 Na) solution does not appear to strongly modulate the transport (Fig. 7, column *f*).

The $[Na^+]_o$ dependence of the Mg^{2+} efflux was studied here by simply changing $[Na^+]_o$ (Fig. 8). Under these

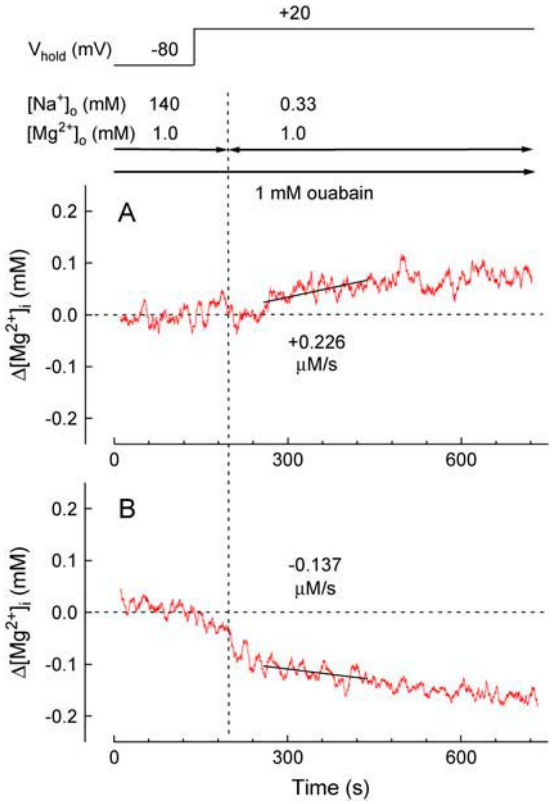

FIGURE 9 Changes in $[Mg^{2+}]_i$ ($\Delta[Mg^{2+}]_i$) on reversal of Na^+ gradient. Panels *A* and *B* show records from two separate experiments in which the myocytes were patch-clamped with the pipette containing either 130 mM Na^+ plus 15 mM K^+ (*A*) or 0 mM Na^+ plus 145 mM K^+ (*B*). Extracellular Na^+ was changed from 140 to 0.33 mM, as indicated above, at the time indicated by a vertical dotted line; the changes in $[Mg^{2+}]_i$ from the baseline (*horizontal dashed lines*) are plotted as a function of time. The holding potential was initially set at −80 mV, and was depolarized to +20 mV ~60 s before the solution exchange. Ouabain (1 mM) was present throughout the experiments. The initial rates of $[Mg^{2+}]_i$ change (the *slopes* of *solid lines*) are indicated below the traces. (*A*) Cell 040403-2, cell capacitance 124 pF, series resistance 24.5 MΩ; cell 120502-1, cell capacitance 109 pF, series resistance 21.6 MΩ.

conditions, $[Na^+]_c$ should be simultaneously changed from essentially zero (Fig. 2 *B*) to various levels depending on $[Na^+]_o$; $[Na^+]_c$ might return to ~12 mM in the presence of 140 mM extracellular Na^+, or to the lower $[Na^+]_c$ levels at a lower $[Na^+]_o$. It is unlikely, however, that changes in $[Na^+]_c$ below the basal level (~12 mM) markedly distort the relation between $[Na^+]_o$ and relative $\Delta[Mg_{tot}]/\Delta t$ (Fig. 8 *B*), as described above. A Hill coefficient of 2.0 and half-maximal activation of 80–90 mM for $[Na^+]_o$ were previously reported for ionomycin-treated myocytes (11,23). The somewhat greater $[Na^+]_o$ estimated for half-maximal activation from ionomycin-treated cells could be due to some unidentified effects of ionomycin on the constituents of the cytoplasm and intracellular organelles. A Hill coefficient close to 2 found in this study (and in the previous study) suggest that two or more Na^+ binding sites are involved in the transport, depending on the degree of cooperativity. These results do not distinguish simple Na^+-Mg^{2+} exchange with more complicated stoichiometries, involving K^+ and Cl^-, as proposed in squid axons ($2Na^+$-$2K^+$-$2Cl^-$-Mg^{2+} exchange; (24)).

Kinetic analysis

To gain information on the mechanism of the extracellular and intracellular Na^+ effects, we analyzed $[Mg^{2+}]_i$ vs. $\Delta[Mg^{2+}]_i/\Delta t$ relations as a function of time; the rates of decrease in $[Mg^{2+}]_i$ ($\Delta[Mg^{2+}]_i/\Delta t$) were estimated at 180-s intervals, and were plotted against $[Mg^{2+}]_i$ at the first point of the fitted line (Fig. 10). The relation could be reasonably described by a Hill-type curve, as previously described (8):

$$\Delta[Mg^{2+}]_i/\Delta t = V_{max} \times X^N/(K^N + X^N), \quad (3)$$

where $X = [Mg^{2+}]_i - K_0$, $K = K_{0.5} - K_0$. K_0 is the threshold $[Mg^{2+}]_i$ at which $\Delta[Mg^{2+}]_i/\Delta t$ is zero and $K_{0.5}$ is $[Mg^{2+}]_i$ that gives the half-maximal value of $\Delta[Mg^{2+}]_i/\Delta t$. V_{max}

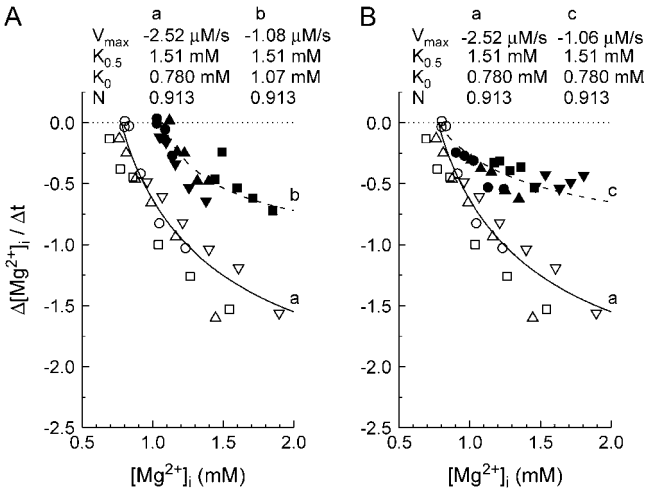

FIGURE 10 Analysis of the relation between $[Mg^{2+}]_i$ and $\Delta[Mg^{2+}]_i/\Delta t$ as a function of time during the $[Mg^{2+}]_i$ decrease. Each symbol represents data from a different myocyte. In panel *A*, data obtained at 140 mM $[Na^+]_o$ in four Na^+-depleted cells (*open symbols*) and four Na^+-loaded cells (*solid symbols*) were compared. Na^+-depleted cells are: cells 100402 (○; patch-clamped with the 145 K/0 Na pipette solution), 083002 (△; incubated in the Na^+-depleting solution and 1 mM ouabain was applied only during the $\Delta[Mg^{2+}]_i/\Delta t$ measurement), 072502 (□; incubated in the Na^+-depleting solution), and 082302 (▽; incubated in the Na^+-depleting solution). Na^+-loaded cells were incubated in the Na^+-loading solution (080102, ▲; 041102, ■; 081602, ▼), except for one patch-clamped with the 130 Na/15 K solution (092702, ●). In panel *B*, data obtained at 140 mM $[Na^+]_o$ in four Na^+-depleted cells (*open symbols*, the same data as shown in *A*) and at 42 mM $[Na^+]_o$ in four Na^+-depleted cells (*solid symbols*) were shown. Na^+-depleted cells exposed to 42 mM $[Na^+]_o$ are cells 091803-2 (●), 091103 (▲), 090103 (■), and 090303 (▼). In panels *A* and *B*, solid curves (*a*) indicate the relation between the initial $[Mg^{2+}]_i$ and the initial $\Delta[Mg^{2+}]_i/\Delta t$ previously obtained with pooled data from many cells (8). Dashed lines (*b* and *c*) show the Hill-type curves fitted to solid symbols with parameter values shown at the top.

denotes the maximum value of $\Delta[Mg^{2+}]_i/\Delta t$. N is the Hill coefficient. In the Na^+-depleted myocytes, the $[Mg^{2+}]_i$ vs. $\Delta[Mg^{2+}]_i/\Delta t$ relation at 140 mM $[Na^+]_o$ (Fig. 10, *A* and *B*, *open symbols*) approximately followed the Hill-type curve that best described the relation between the initial $[Mg^{2+}]_i$ and the initial $\Delta[Mg^{2+}]_i/\Delta t$ in the previous study (*A* and *B*, *solid curves* marked *a*); the fitted parameter values were 0.78 mM for K_0, 1.51 mM for $K_{0.5}$, −2.52 μM/s for V_{max}, and 0.913 for N (8). In the myocytes loaded with Na^+ for 3 h, the relation was clearly shifted to the right (*A*, *solid symbols*); the fitted curve had a higher threshold (K_0 increased by 0.29 mM) and a lower maximum transport rate (V_{max} decreased by 57%), whereas other parameter values were kept constant (*A*, *dashed curve* marked *b*). In the Na^+-depleted myocytes, values of the $\Delta[Mg^{2+}]_i/\Delta t$ at 42 mM $[Na^+]_o$ (*B*, *solid symbols*) were well explained by simple scaling of the curve at 140 mM $[Na^+]_o$; the dashed line in panel *B* (*c*) indicates a lower V_{max} (by 58%) whereas other parameter values were unchanged.

Although the effect of low $[Na^+]_o$ can be explained simply by reduction of the driving force (i.e., a decrease in V_{max}; Fig. 10 *B*), the effect of high $[Na^+]_c$ appears to be more complicated. As shown in Fig. 10 *A*, intracellular Na^+ loading caused a shift of the threshold $[Mg^{2+}]_i$ above which the Mg^{2+} efflux was strongly activated. Günther et al. (25) found a similar threshold for the Mg^{2+} efflux in chicken erythrocytes, and proposed the existence of an apparent ''gating'' process in addition to Michaelis-Menten kinetics. Our results (Fig. 10 *A*) are consistent with the ''gating'' process, and suggest that intracellular Na^+ exerts its inhibitory effect on the Mg^{2+} efflux by inhibition of the ''gating'', in addition to a reduction of the transport rate of Michaelis-Menten kinetics. For the mechanism of the reduced transport rate, these data obtained within the limited $[Mg^{2+}]_i$ range (<2 mM) do not allow us to determine whether the increase in $[Na^+]_c$ affects only the driving force (a decrease in V_{max}; Fig. 10 *A*, *dashed curve* marked *b*) or it also interferes with the binding of internal Mg^{2+} (an increase in $K_{0.5}$; not shown). The measurements of $\Delta[Mg^{2+}]_i/\Delta t$ at much higher $[Mg^{2+}]_i$ ranges will be helpful to clarify these two possibilities.

Mg^{2+} influx with reversal of the Na^+ gradient

If the Mg^{2+} transport is driven only by electrochemical gradient of Na^+, it is expected that Mg^{2+} may be transported in the opposite direction upon a sufficiently strong reversal of the Na^+ gradient. Even in erythrocytes, in which the Na^+-Mg^{2+} exchange is characterized more clearly than in other cell types, experimental results about reversibility of the Mg^{2+} transport remain controversial. For example, Na^+-dependent Mg^{2+} uptake is observed at low $[Na^+]_o$ in ferret red cells (26), but it is not detected in Na^+-loaded human erythrocytes (27) and rat erythrocytes (22). In cardiac myocytes studied with furaptra, Handy et al. (10) reported a gradual elevation of $[Mg^{2+}]_i$ when $[Mg^{2+}]_o$ was raised to 5 mM and $[Na^+]_o$ was removed in Ca^{2+}-free solution at 37°C. It is possible, however, that a passive Mg^{2+} influx pathway, rather than the reversed Na^+-Mg^{2+} exchange, plays a role when a rise of $[Mg^{2+}]_i$ is observed without control of membrane potential.

A rise of $[Mg^{2+}]_i$ was hardly observed with a short-term superfusion with a Na^+- and Ca^{2+}-free solution containing 30 mM Mg^{2+} at 25°C (11,28). In this study, we detected a small rise of $[Mg^{2+}]_i$ on removal of extracellular Na^+ only in cells that had been heavily loaded with Na^+ at 140 mM $[Na^+]_o$ plus ouabain combined with intracellular perfusion by 130 mM $[Na^+]_p$ (Fig. 10). With intracellular perfusion with 0 mM $[Na^+]_p$, on the other hand, removal of extracellular Na^+ caused a monotonic reduction of $[Mg^{2+}]_i$, which could be attributed to an artifact in furaptra due to the loss of the remaining Na^+ from the cell (see above). Even under the maximized concentration gradient of Na^+, the rate of rise in $[Mg^{2+}]_i$ (i.e., Mg^{2+} influx rate) was much smaller than the rate of Mg^{2+} efflux, which could be explained by asymmetry of the Mg^{2+} transport (i.e., fast turnover for Mg^{2+} efflux and very limited turnover rate in the opposite direction) proposed by Günther et al. (22) for erythrocytes. Additional studies are necessary to fully characterize the Mg^{2+} influx observed here.

Mg^{2+} flux across the cell membrane

A typical value of $\Delta[Mg_{tot}]/\Delta t$ in the physiological condition in Table 2 is ~2.5 μM/s and V_{max} may be as high as ~5 μM/s at very high $[Mg^{2+}]_c$ (8). Assuming a cell surface area/volume ratio of 0.63 μm^{-1} (surface area 1.23×10^4 μm^2 (29); volume 1.95×10^4 μm^3 (30)) and a cytoplasm/cell volume ratio of 0.5 (31), values of $\Delta[Mg_{tot}]/\Delta t$ could be converted to transmembrane Mg^{2+} fluxes; $\Delta[Mg_{tot}]/\Delta t$ of 2.5–5 μM/s would correspond to a membrane flux of 0.2–0.4 pmol/cm^2·s (i.e., 0.2–0.4 pmol/μF s). This value may be compared with Ca^{2+} flux of the Na^+-Ca^{2+} exchange. In guinea pig ventricular myocytes, Miura and Kimura (32) reported ~30 pmol/cm^2 s (i.e., ~3 μA/μF; see their Fig. 6) for the physiological V_{max} of the Ca^{2+} flux at 35–37°C, which corresponds to ~7 pmol/cm^2 s at 25°C assuming Q_{10} of 4 for the Na^+-Ca^{2+} exchanger (33). In rat ventricular myocytes, in which density of the Na^+-Ca^{2+} exchanger protein (and amplitude of the exchange current) is five times smaller than in guinea pigs (34), the physiological V_{max} value may be 1.4 pmol/cm^2 s. Thus, the Mg^{2+} flux by the putative Na^+-Mg^{2+} exchange may be several times smaller than the Ca^{2+} flux carried by the Na^+-Ca^{2+} exchanger, if compared in the same animal species at 25°C.

In conclusion, this study clearly demonstrates that elevated intracellular Na^+ can strongly inhibit the Mg^{2+} efflux (and even reverse the transport). At physiological levels of $[Na^+]_c$ (~10 mM) and $[Na^+]_o$ (~140 mM), however, small changes in $[Na^+]_c$ and $[Na^+]_o$ would not strongly modulate

the rate of Mg^{2+} transport. During metabolic inhibition, however, a rise of $[Na^+]_c$ to much higher levels is expected (35); this might inhibit the Mg^{2+} efflux and might partly contribute to the rise of $[Mg^{2+}]_c$ found in ischemic hearts (36).

We thank Dr. Stephen M. Baylor for helpful comments and Ms. Mary Shibuya for reading the manuscript.

This work was supported by a Grant-in-Aid for Scientific Research from the Japan Society for the Promotion of Science (No. 14370016) and ''High-Tech Research Center'' Project for Private Universities, a matching fund subsidy from the Ministry of Education, Culture, Sports, Science and Technology, 2003–2007.

REFERENCES

1. Agus, Z. A., and M. Morad. 1991. Modulation of cardiac ion channels by magnesium. *Annu. Rev. Physiol.* 53:299–307.
2. Wang, M., M. Tashiro, and J. R. Berlin. 2004. Regulation of L-type calcium current by intracellular magnesium in rat cardiac myocytes. *J. Physiol. (Lond.).* 555:383–396.
3. Tashiro, M., C. I. Spencer, and J. R. Berlin. 1999. Modulation of cardiac excitation-contraction coupling by cytosolic $[Mg^{2+}]$. *Biophys. J.* 76:A461.
4. Donaldson, S. K. B., P. M. Best, and G. L. Kerrick. 1978. Characterization of the effects of Mg^{2+} on Ca^{2+}- and Sr^{2+}-activated tension generation of skinned rat cardiac fibers. *J. Gen. Physiol.* 71: 645–655.
5. Fabiato, A. 1993. Calcium-induced release of calcium from the cardiac sarcoplasmic reticulum. *Am. J. Physiol.* 245:C1–C14.
6. Konishi, M., and J. R. Berlin. 1993. Ca transients in cardiac myocytes measured with a low affinity fluorescent indicator, furaptra. *Biophys. J.* 64:1331–1343.
7. Buri, A., and J. A. S. McGuigan. 1990. Intracellular free magnesium and its regulation, studied in isolated ferret ventricular muscle with ion selective microelectrodes. *Exp. Physiol.* 75:751–761.
8. Tursun, P., M. Tashiro, and M. Konishi. 2005. Modulation of Mg^{2+} efflux from rat ventricular myocytes studied with the fluorescent indicator furaptra. *Biophys. J.* 88:1911–1924.
9. Romani, A., C. Marfella, and A. Scarpa. 1993. Regulation of magnesium uptake and release in the heart and in isolated ventricular myocytes. *Circ. Res.* 72:1139–1148.
10. Handy, R. D., I. F. Gow, D. Ellis, and P. W. Flatman. 1996. Na-dependent regulation of intracellular free magnesium concentration in isolated rat ventricular myocytes. *J. Mol. Cell. Cardiol.* 28:1641–1651.
11. Tashiro, M., and M. Konishi. 2000. Sodium gradient-dependent transport of magnesium in rat ventricular myocytes. *Am. J. Physiol.* 279:C1955–C1962.
12. Flatman, P. W. 1991. Mechanisms of magnesium transport. *Annu. Rev. Physiol.* 53:259–271.
13. Romani, A., and A. Scarpa. 2000. Regulation of cellular magnesium. *Front. Biosci.* 5:d720–d734.
14. McGuigan, J. A. S., H. Y. Elder, D. Günzel, and W.-R. Schlue. 2002. Magnesium homeostasis in heart: a critical reappraisal. *J. Clin. Basic Cardiol.* 5:5–22.
15. Tashiro, M., and M. Konishi. 2003. Intracellular Na^+ inhibits Mg^{2+} efflux from rat ventricular myocytes. *Jpn. J. Physiol.* 53:S147.
16. Tashiro, M., P. Tursun, and M. Konishi. 2002. Effects of membrane potential on Na^+-dependent Mg^{2+} extrusion from rat ventricular myocytes. *Jpn. J. Physiol.* 52:541–551.
17. Watanabe, M., and M. Konishi. 2001. Intracellular calibration of the fluorescent Mg^{2+} indicator furaptra in rat ventricular myocytes. *Pflugers Arch.* 442:35–40.
18. Tajima, Y., K. Ono, and N. Akaike. 1996. Perforated patch-clamp recording in cardiac myocytes using cation-selective ionophore gramicidin. *Am. J. Physiol.* 271:C524–C532.
19. Donoso, P., J. G. Mill, S. C. O'Neill, and D. A. Eisner. 1992. Fluorescence measurements of cytoplasmic and mitochondrial sodium concentration in rat ventricular myocytes. *J. Physiol. (Lond.).* 448:492–509.
20. Harrison, S. M., J. E. Frampton, E. McCall, M. R. Boyett, and C. H. Orchard. 1992. Contraction and intracellular Ca^{2+}, Na^+, and H^+ during acidosis in rat ventricular myocytes. *Am. J. Physiol.* 262:C348–C357.
21. Borin, M. L., W. F. Goldman, and M. P. Blaustein. 1993. Intracellular free Na^+ in resting and activated A7r5 vascular smooth muscle cells. *Am. J. Physiol.* 264:C1513–C1524.
22. Günther, T., J. Vormann, and V. Höllriegl. 1990. Characterization of Na^+-dependent Mg^{2+} efflux from Mg^{2+}-loaded rat erythrocytes. *Biochim. Biophys. Acta.* 1023:455–461.
23. Konishi, M., M. Tashiro, M. Watanabe, T. Iwamoto, M. Shigekawa, and S. Kurihara. 2001. Cell membrane transport of magnesium in cardiac myocytes and CCL39 cells expressing the sodium-calcium exchanger. *In* Advances in Magnesium Research: Nutrition and Health. Y. Rayssiguier, A. Mazur, and J. Durlach, editors. John Libbey & Co., London, UK. 53–57.
24. Rasgado-Flores, H., H. Gonzalez-Serratos, and J. DeSantiago. 1994. Extracellular Mg^{2+}-dependent Na^+, K^+, and Cl^- efflux in squid giant axons. *Am. J. Physiol.* 266:C1112–C1117.
25. Günther, T., J. Vormann, and R. Förster. 1984. Regulation of intracellular magnesium by Mg^{2+} efflux. *Biochem. Biophys. Res. Commun.* 119:124–131.
26. Flatman, P. W., and L. M. Smith. 1991. Sodium-dependent magnesium uptake by ferret red cells. *J. Physiol. (Lond.).* 443:217–230.
27. Lüdi, H., and H. J. Schatzmann. 1987. Some properties of a system for sodium-dependent outward movement of magnesium from metabolizing human red blood cells. *J. Physiol. (Lond.).* 390:367–382.
28. Steele, M. G., P. W. Flatman, and D. Ellis. 2003. Temperature dependence of Mg^{2+} transport in isolated ventricular myocytes. *J. Physiol. (Lond.).* 547P:C18.
29. Levi, J. A. 1992. The electrogenic sodium-potassium pump and passive sodium influx of isolated guinea-pig ventricular myocytes. *J. Cardiovasc. Electrophysiol.* 3:225–238.
30. Boyett, M. A., J. E. Frampton, and M. S. Kirby. 1991. The length, width and volume of isolated rat and ferret ventricular myocytes during twitch contractions and changes in ionic strength. *Exp. Physiol.* 76: 259–270.
31. Sipido, K. R., and W. G. Wier. 1991. Flux of Ca^{2+} across the sarcoplasmic reticulum of guinea-pig cardiac cells during excitation-contraction coupling. *J. Physiol. (Lond.).* 435:605–630.
32. Miura, Y., and J. Kimura. 1989. Sodium-calcium exchange current. Dependence of internal Ca and Na and competitive binding of external Na and Ca. *J. Gen. Physiol.* 93:1129–1145.
33. Kimura, J., S. Miyamae, and A. Noma. 1987. Identification of sodium-calcium exchange current in single ventricular cells of guinea-pig. *J. Physiol. (Lond.).* 384:199–222.
34. Kimura, J., S. Ohkubo, and I. Matsuoka. 1997. Comparison of cardiac Na^+-Ca^{2+} exchange protein in guinea-pig and rat by western blot. *Jpn. J. Physiol.* 47:S58.
35. Satoh, H., H. Hayashi, H. Katoh, H. Terada, and A. Kobayashi. 1995. Na^+/H^+ and Na^+/Ca^{2+} exchange in regulation of $[Na^+]_i$ and $[Ca^{2+}]_i$ during metabolic inhibition. *Am. J. Physiol.* 268:H1239–H1248.
36. Murphy, E., C. Steenbergen, L. A. Levy, B. Raju, and R. E. London. 1989. Cytosolic free magnesium levels in ischemic rat heart. *J. Biol. Chem.* 264:5622–5627.
37. Martell, A. E., and R. M. Smith. 1974. Critical Stability Constants, Vol. 1. Plenum Publishing, New York, NY.